Adsorption/Desorption of Tetrahydrothiophene from Natural Gas onto Granular and Fiber−Cloth Activated Carbon for Fuel Cell Applications

ARTICLE *in* ENERGY & FUELS · FEBRUARY 2009

Impact Factor: 2.79 · DOI: 10.1021/ef800757u

2 AUTHORS, INCLUDING:

Pierre Le Cloirec
Ecole Nationale Supérieure de Chimie de R…

312 PUBLICATIONS **6,399** CITATIONS

SEE PROFILE

Article

Adsorption/Desorption of Tetrahydrothiophene from Natural Gas onto Granular and Fiber-Cloth Activated Carbon for Fuel Cell Applications

Benoit Boulinguiez, and Pierre Le Cloirec

Energy Fuels, **2009**, 23 (2), 912-919• DOI: 10.1021/ef800757u • Publication Date (Web): 13 January 2009

Adsorption/Desorption of Tetrahydrothiophene from Natural Gas onto Granular and Fiber-Cloth Activated Carbon for Fuel Cell Applications

Benoit Boulinguiez* and Pierre Le Cloirec

École Nationale Supérieure de Chimie de Rennes, CNRS, UMR 6226, Avenue du Général Leclerc, CS50837, 35708 Rennes CEDEX 7, France and Université européenne de Bretagne, 12 Avenue Janvier, 35000 Rennes, France

Received September 9, 2008. Revised Manuscript Received November 21, 2008

Natural gas with a high methane concentration is an important source of primary fuel for fuel cells, although it contains sulfur compounds, such as tetrahydrothiophene (THT), known as a poison for the fuel cell catalyst parts. Desulfurization of natural gas fuel in ambient conditions is thus essential before it enters the reforming process. Adsorptive removal of THT from natural gas was tested on three different activated carbon materials: two granular materials (GAC) and one fiber-cloth material (ACFC). The adsorption isotherms, fitted by nonlinear regression procedures, of the THT onto the materials showed the promising adsorptive capacity of the ACFC compared to the GAC, validated by adsorption kinetics in favor of ACFC. The continuous adsorption of THT from the natural gas pipe determined the adsorption capacity of the ACFC (100 mg g^{-1}). Thermal regeneration investigations were carried out on the ACFC to confirm the adsorption/desorption capacity and process feasibility of the material. The formation of thiophene and elemental sulfur was noted as catalytic products of the oxidative reaction of THT during the thermal desorption from the activated carbon material. The Joule-effect heating used as an electro-regeneration process for the ACFC offers a great choice in terms of the desorption operating procedure and highlights the potential of this material for the desulfurization of natural gas for fuel cell applications.

Introduction

Energy companies are facing the challenge of producing increasingly cleaner energies because of worldwide environmental mandates. Fuel cells present high fuel−electricity conversion efficiencies and low levels of pollutant emission and thus fulfill these environmental requirements.[1] A fuel cell transforms the oxidation energy of a fuel into electricity. Because this process does not follow Carnot's theorem, higher energy efficiencies are expected: 40−50% in electrical energy and 80−5% in total energy (electricity and heat production). Different kinds of fuel cells have been developed for several applications (automotive and stationary power) depending upon the nominal power required.[2] For most applications, hydrogen is the convenient fuel produced from a primary fuel, such as methane. The widespread distribution grids of natural gas in many countries represent a consequent and cost-effective source of primary fuel for fuel cells.

Natural gas contains sulfur compounds, such as THT (variables and acronyms are defined in the Nomenclature), added deliberately as an odorant to detect gas leakage (French national gas grid, for instance). THT is not corrosive and does not cause irritant responses contrary to the ethanthiol. The Nagata odor threshold of THT is 0.00062 ppm(v) for a 2.4 kPa vapor pressure at 25 °C; thus, it is considered as a interesting gas indicator option to the use of ethantiol as an odorant in natural gas. The poisoning effect of sulfur components in the catalytic reaction and especially at the fuel cell anode has been pointed out even at low levels of sulfur compounds.[3−6] Furthermore, the trend in fuel cell development to reduce operating temperature thermodynamically improves sulfur adsorption and thus the poisoning of catalysts.[4] Therefore, the removal of sulfur compounds present in natural gas is the essential first step to produce a methane-rich fuel stream before the steam-reforming process.

It is achieved either by HDS or adsorption−desorption cycles. HDS has been the traditional preprocessing method to achieve desulfurization, despite some restrictions. The process requires hydrogen and a consistent energy supply because of the elevated temperatures and pressures required. As a consequence, fuel desulfurization research has focused on a low-temperature adsorption process that is supported by either activated carbon or zeolite.[7−15] Adsorption processes have the advantage of removing sulfur compounds at concentrations below 1 ppm(v).

* To whom correspondence should be addressed. E-mail: benoit.boulinguiez@ensc-rennes.fr.

(1) Pomfret, M.; Demircan, O.; Sukeshini, A.; Walker, R. *Environ. Sci. Technol.* **2006**, *40*, 5574–5579.

(2) Basu, S. *Recent Trends in Fuel Cell Science and Technology*; Springer: New York, 2007; p 260.

(3) Matsuzaki, Y.; Yasuda, I. *Solid State Ionics* **2000**, *132*, 261–269.

(4) Cheng, Z.; Zha, S.; Liu, M. *J. Power Sources* **2007**, *172*, 688–693.

(5) Foger, K.; Ahmed, K. *J. Phys. Chem. B* **2005**, *109*, 2149–2154.

(6) Norheim, A.; Warnhus, I.; Brostrom, M.; Hustad, J.; Vik, A. *Energy Fuels* **2007**, *21*, 1098–1101.

(7) de Wild, P.; Nyqvist, R.; de Bruijn, F.; Stobbe, E. *J. Power Sources* **2006**, *159*, 995–1004.

(8) Lee, D.; Ko, E.-Y.; Lee, H. C.; Kim, S.; Park, E. D. *Appl. Catal., A* **2008**, *334*, 129–136.

(9) Ko, C.; Song, H.-I.; Park, J.-H.; Han, S.-S.; Kim, J.-N. *Korean J. Chem. Eng.* **2007**, *24*, 1124–1127.

(10) Kang, S.-H.; Bae, J.-W.; Kim, H.-T.; Jun, K.-W.; Jeong, S.-Y.; Chary, K. V. R.; Yoon, Y.-S.; Kim, M.-J. *Energy Fuels* **2007**, *21*, 3537–3540.

(11) Israelson, G. *J. Mater. Eng. Perform.* **2004**, *13*, 282–286.

(12) Wakita, H.; Tachibana, Y.; Hosaka, M. *Microporous Mesoporous Mater.* **2001**, *46*, 237–247.

10.1021/ef800757u CCC: $40.75
Published on Web 01/13/2009

Between the two absorbent materials, zeolites quickly attracted the scientific community's attention because of a wider range of species and higher sulfur adsorption capacities than activated carbon, as reported by researchers in comparative studies.[7,11,14] Therefore, in the last 10 years, most scientific information has been oriented toward the presentation and benchmark tests of zeolites for sulfur removal.[8−13,15]

However, although zeolites usually present adsorption capacities higher than AC, the regeneration of such a material represents a financial barrier from a global process overview. Authors report a complete desorption temperature between 400 and 500 °C, whereas AC materials exhibit a regeneration temperature close to 200 °C for sulfur compounds.[8,13,14] Considering this valuable aspect of low-temperature regeneration, AC may represent an option worth investigating in desulfurization by adsorption. In particular, ACFC could be a promising material for such operations. Indeed, ACFC present the process opportunity of Joule-effect heating[16−19] and adsorption properties similar to regular activated carbon granular material applied in treatment processes.[20−22] Therefore, adsorption and electrothermal desorption cycles on ACFC may provide a new opportunity for cost-effective desulfurization by adsorption for fuel cell applications. Nonetheless, the rising interest in and development of the ACFC process requires prior investigations, such as adsorption capacity, regeneration feasibility, and byproduct formation. The latter is scarcely reported in regeneration studies, although activated carbon has a known catalytic activity because of metal traces, especially with sulfur compounds, which may react at elevated temperature in the presence of catalysts.[23] The desorption conditions may fulfill the thermodynamic requirements for the reaction of sulfur compounds and thus generate undesirable components.

This study has three objectives: (i) to compare the THT adsorption kinetic and capacity between an ACFC and two commercial GAC in the natural gas atmosphere, (ii) to investigate the adsorption−desorption cycle process feasibility and behavior with the ACFC, and (iii) to investigate byproduct formation during desorption cycles of ACFC.

Materials and Methods

Adsorbents. All AC materials are commercial products manufactured by Pica (Saint-Maurice, France) or Charcoal Cloth International (CCI, U.K.). An identical conditioning procedure was applied to all of the materials. GAC and ACFC were washed several times with deionized water and acetone prior to a 12 h soaking period in deionized water to remove pollutant traces from the manufacturing or storage step. The materials were then dried at 150 °C overnight. Some properties of the adsorbent materials are listed in Table 1. Porous analyses were carried out by adsorption−desorption of nitrogen at 77 K with the ASAP 2010 (Micromeritics). The samples were degassed during 72 h before measurement. For the specific surface area, the Brunauer−Emmett−Teller (BET) theory is used, and for the microporosity, the Howarth−Kawazoe theory was applied.

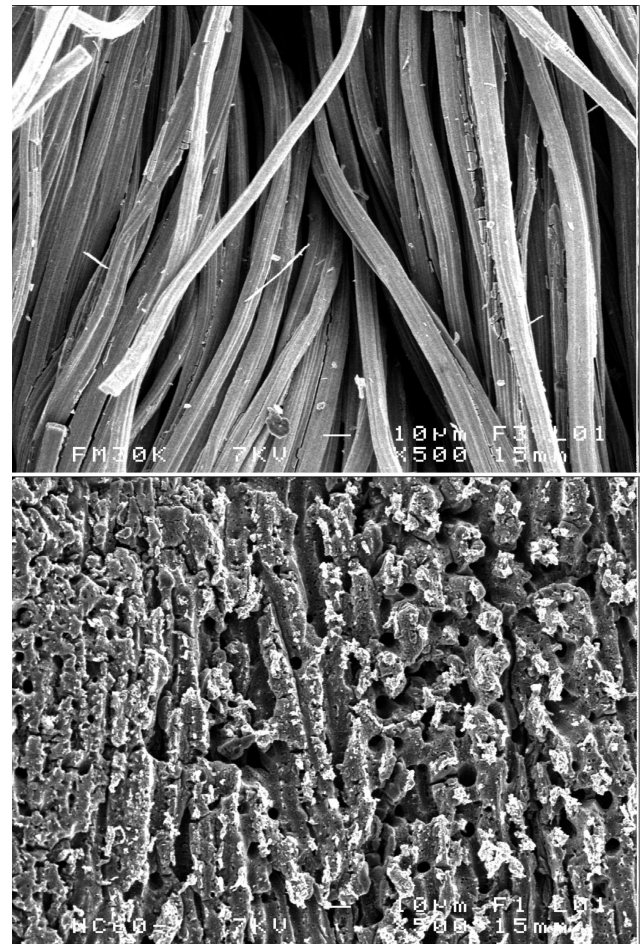

Figure 1. SEM pictures of virgin FM30K (above) and NC60 (below), enlargement ×500.

Table 1. Main Characteristics of the Adsorbents

name	Picabiol	NC60	Zorflex FM30K
manufacturer	Pica	Pica	CCI
original material	wood	coconut	viscose
form	grain	grain	fiber cloth
porous volume ($cm^3\ g^{-1}$)	0.99	0.59	0.49
S_{BET} ($m^2\ g^{-1}$)	1600	1250	1150
microporous volume (%)	63	87	75
median pore width (nm)	0.71	0.58	0.34
grain diameter/thickness (mm)	1.16	1.22	0.40

Microscopic observations were carried out on AC materials with a JEOL JSM 6301F (Figure 1) and a JEOL JSM 6400 coupled with an energy-dispersive system (X-ray spectrometer) for elemental analysis of the material after adsorption−desorption cycles.

Adsorption Equilibrium and Kinetics. Adsorption or kinetics in batch reactors is a classical experimental procedure to evaluate the pollutant removal from the fluid phase. A common isotherm method was applied; fixed known weighed amounts of adsorbent were suspended in identical batch reactors filled with natural gas, to which different weighed amounts of liquid THT were added, volatilized, and continuously stirred. The initial THT concentration in the reactor because of the natural gas was negligible (0.1 mg) compared to the added amount of liquid pure THT (in the lowest case, 10 mg). All reactors were placed in a thermostatted bath regulated at 25 ± 0.2 °C for 20 h. The equilibrium concentration range investigated was 10−200 mg m^{-3}. Gas samples were

(13) Satokawa, S.; Kobayashi, Y.; Fujiki, H. *Appl. Catal., B* **2005**, *56*, 51–56.
(14) Roh, H.-S.; Jun, K.-W.; Kim, J.-Y.; Kim, J.-W.; Park, D.-R.; Kim, J.-D.; Yang, S.-S. *J. Ind. Eng. Chem.* **2004**, *10*, 511–515.
(15) Novochinskii, I.; Song, C.; Ma, X.; Liu, X.; Shore, L.; Lampert, J.; Farrauto, R. *Energy Fuels* **2004**, *18*, 576–583.
(16) Subrenat, A.; Baléo, J. N.; Le Cloirec, P.; Blanc, P. E. *Carbon* **2001**, *39*, 707–716.
(17) Subrenat, A.; Le Cloirec, P. *J. Environ. Eng.* **2003**, *129*, 1077–1084.
(18) Sullivan, P. D.; Rood, M. J.; Grevillot, G.; Wander, J. D.; Hay, K. J. *Environ. Sci. Technol.* **2004**, *38*, 4865–4877.
(19) Ramos, M. E.; Gonzalez, J. D.; Bonelli, P. R.; Cukierman, A. L. *Ind. Eng. Chem. Res.* **2007**, *46*, 1167–1173.
(20) Le Cloirec, P.; Brasquet, C.; Subrenat, E. *Energy Fuels* **1997**, *11*, 331–336.
(21) Brasquet, C.; Le Cloirec, P. *Carbon* **1997**, *35*, 1307–1313.
(22) Brasquet, C.; Bourges, B.; Le Cloirec, P. *Environ. Sci. Technol.* **1999**, *33*, 4226–4231.
(23) Desikan, P.; Amber, C. *Can. J. Chem.* **1964**, *42*, 843–850.

manually injected into a gas chromatograph (Agilent 6890) equipped with a flame photometric detector.

The different experimental isotherms are modeled according to the Langmuir model equation as follows:

$$q_e = \frac{q_m b C_e}{1 + bC_e} \quad (1)$$

The Freundlich-type model is not reported here because, although it remains a widely used descriptive model, it does not give any limit to adsorption capacity, making the amount adsorbed go to infinity when the concentration increases. Thus, the Freundlich model is only applicable over limited ranges of adsorption, whereas the Langmuir isotherm model respects the Henry-type equation at low adsorption capacity and the limit of saturation. Therefore, for a two-adjustable-parameter model, the Langmuir model is preferred in our study.

The assessment of the Langmuir model parameter was the subject of a previous study.[24] Five different methods were used to assess these parameters. The common linear transformations,[25] such as the Lineweaver−Burk, the Hanes−Wolf, and the Eadie−Hofstee, exhibited their limit because they created distortions in the error distribution of the data and yielded different parameter estimates. A new nonlinear regression approach was studied, derived from the expression of the equilibrium solid-phase concentration as a function of the initial conditions only. The equation is as follows:

$$q_e = \frac{V - \zeta + bmq_m + C_0 Vb}{2bm} \quad (2)$$

with

$$\zeta = \sqrt{C_0^2 V^2 b^2 + 2C_0 V^2 b - 2C_0 Vb^2 mq_m + V^2 + 2Vbmq_m + b^2 m^2 q_m^2}$$

This alternative nonlinear regression procedure showed interesting fitting results that have been developed further with the R software. Therefore, fitting results reported in the present paper are those obtained by the alternative nonlinear regression method with the R software. The fitting quality of the model is evaluated here by four error functions: the HYBRID, the r^2, the ARE, and the s_{RE}.[24]

For the kinetic study, an identical procedure was applied to each AC. A total of 250 mg of AC was suspended in the reactor filled with natural gas, to which 30 mg of pure liquid THT was added, volatilized, and continuously stirred at 25 ± 0.2 °C. Gas samples were withdrawn at regular intervals with a 250 μL gastight syringe and injected into a gas chromatograph (Thermo Focus) equipped with a flame ionization detector.

The initial adsorption coefficient γ,[26] the external film mass-transfer coefficient k_sA,[27] and the internal diffusion coefficient of Weber K_W[28] are used to quantify the kinetic adsorption behavior of an adsorbent.

The γ coefficient is determined by the initial adsorption kinetic, which could be described by the Adam, Bohart, and Thomas relation. The derivative equation is as follows:

$$\frac{dq}{dt} = K_{ABT} C(q_m - q) - K'_{ABT} q \quad (3)$$

At the initial stage of the adsorption reaction, when $t \to 0$, $q \to 0$, and $C \to C_0$, eq 3 could be reformulated as

$$\gamma = -K_{ABT} q_m = -\frac{V}{C_0 m}\left(\frac{dC}{dt}\right)_{t \to 0} \quad (4)$$

The external film mass-transfer coefficient k_sA is determined by the linear driving force for the mass-transfer relation as follows:[29]

$$V\frac{dC}{dt} = -k_s A(C - C_s) \quad (5)$$

At the initial stage of the adsorption reaction, when $t \to 0$, $C_s \to 0$, and $C \to C_0$, eq 5 could be reformulated as

$$-\ln\frac{C}{C_0} = \frac{k_s A}{V} t \quad (6)$$

When the adsorption kinetics are essentially due to internal diffusion, the gas-phase concentration variation is proportional to the square root of time (Fick law). This is considered valid when the adsorbed quantity is less than 20% of the maximal adsorption capacity. Hence, the internal diffusion coefficient of Weber K_W is obtained from the following relation:

$$C = C_0 - K_W t^{1/2} \quad (7)$$

Actually, the K_W coefficient groups the porous diffusion coefficient and the surface-transfer coefficient.

Data sets in both adsorption equilibrium and kinetics parts present a constant coefficient of variation below 10% over the whole concentration range investigated.

Adsorption−Desorption Cycles. The THT saturation of the ACFC layer with natural gas was ensured in a continuous laboratory-scale flow reactor fed by natural gas from the national grid until the outflow concentration reached the inlet value. The ACFC layer was 2.5 cm in diameter and 0.4 mm in thick. The gas velocity in the adsorption module was 250 m h^{-1}. The THT concentration in the natural gas was measured at 51 mg m^{-3} [14 ppm(v)], and adsorption was performed at room temperature, 25 ± 0.2 °C. The adsorption and thermal desorption cycles of a saturated sample of the ACFC layer were investigated using different techniques.

Thermogravimetric measurements (Shimatzu 50) were used to determine the temperature desorption range and behavior of saturated ACFC samples. The sample weight range was 15−20 mg. This desorption process occurred under nitrogen flow at 50 mL min^{-1}, with a temperature gradient of 5 °C min^{-1}.

Saturated ACFC samples were placed in sealed vials and desorbed at the selected temperature (from 60 to 210 °C) in a headspace thermal desorber (PerkinElmer TurboMatrix 40 Trap). The echelon desorption time was fixed at 10 min. Then, an aliquot of the headspace was automatically withdrawn, injected, and measured with a GC/MS (PerkinElmer Clarus 500) to identify the molecule structure and the range of desorbed compounds from the ACFC.

The sulfur mass balance was monitored during adsorption−desorption cycles. The temperature effect (from 20 to 400 °C) on the desorption performance was investigated on a saturated ACFC layer to corroborate the results highlighted by the thermogravimetric measurements.

Finally, a nondestructive inspection of the ACFC by SEM at 10^{-5}−10^{-6} torr with the JEOL JSM 6400 coupled with X-ray measurements was carried out to assess the long-term modification of the material after 10 adsorption−desorption cycles. The last desorption occurred at 300 °C overnight to ensure full desorption of the sample. The microscopy and X-ray analysis covered three distinct areas of the ACFC sample to reduce the bias of a local modification of the material.

Results and Discussion

Adsorption Isotherm. Adsorption isotherms of THT on the three AC materials and their respective models are given in Figure 2. All isotherms are type I, demonstrating favorable

(24) Boulinguiez, B.; Le Cloirec, P.; Wolbert, D. *Langmuir* **2008**, *24*, 6420–6424.
(25) Persoff, P.; Thomas, J. F. *Soil Sci. Soc. Am. J.* **1988**, *52*, 886–889.
(26) Baudu, M.; Le Cloirec, P.; Martin, G. *Water Sci. Technol.* **1991**, *23*, 1659–1666.
(27) McKay, G.; Bino, M. J. *Water Res.* **1988**, *22*, 279–286.
(28) Sphan, H.; Under, E. S. *Chem. Eng. Sci.* **1975**, *30*, 529–537.
(29) Kadirvelu, K.; Faur-Brasquet, C.; Le Cloirec, P. *Langmuir* **2000**, *16*, 8404–8409.

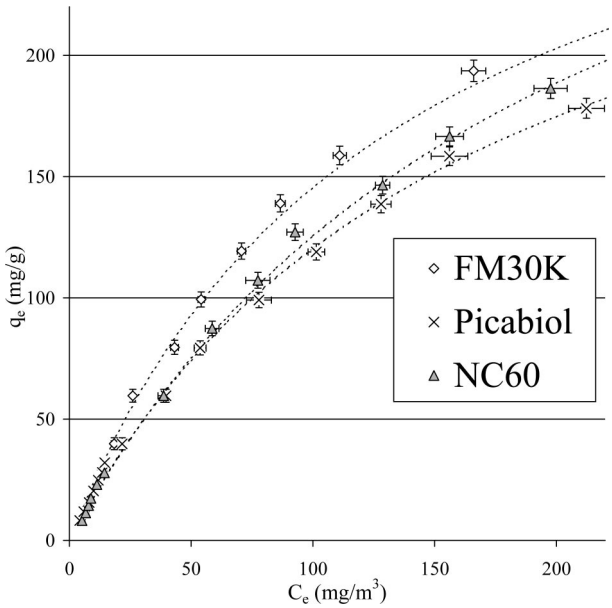

Figure 2. Adsorption isotherms of THT onto AC; $T = 25 \pm 0.2$ °C; contact time for each point = 20 h.

Table 2. Isotherm Model Results and Kinetic Coefficients

parameters	Picabiol	NC60	FM30K
q_m	310	354	342
b	0.0064	0.0057	0.0072
HYBRID	0.19	0.14	0.15
r^2	0.998	0.999	0.999
ARE (%)	0.9	1.3	−3.5
s_{RE}	0.01	0.11	0.07
γ ($\times 10^9$)	2.86	2.52	5.43
k_sA ($\times 10^6$)	1.37	1.25	1.90
K_W	3.52	4.44	3.84

adsorption of THT present in the natural gas matrix.[30] The parameter assessment results are shown in Table 2. The adsorption experimental data are satisfactorily fitted by the Langmuir model. This is confirmed by the good values obtained with the different error functions. Discussion of adsorption capacities with these assessed parameters is therefore valuable.

The maximum adsorption capacity is of the same order of magnitude, whichever adsorbent is considered. The NC60 exhibits a slightly higher maximum adsorption capacity than the FM30K, although the latter adsorbs more THT at low concentrations than any GAC. These aspects are emphasized by the model parameter values: for the NC60, the value of q_m is the highest, yet for the FM30K, the value of b is the highest and compensates the intermediate q_m value, thus explaining the highest adsorbed amount of THT at low concentrations. Because the saturation of an adsorbent is rarely reached in applications (the adsorbent is generally regenerated before that situation occurs), the FM30K exhibits the most interesting adsorption capacity for our target applications.

The correlation between the adsorption capacity and the inherent physical characteristics of the adsorbents is delicate. Indeed, neither the FM30K nor the NC60 present the highest microporous volume, the highest porous volume, or the highest BET surface. Thus, adsorption of THT in natural gas onto activated carbon seems to be driven by the complex chemical structure of the adsorbent, which influences the interaction with the adsorbate.[30]

(30) Bansal, R. C.; Meenakshi, G. *Activated Carbon Adsorption*; CRC Press: Boca Raton, FL, 2005; p 520.

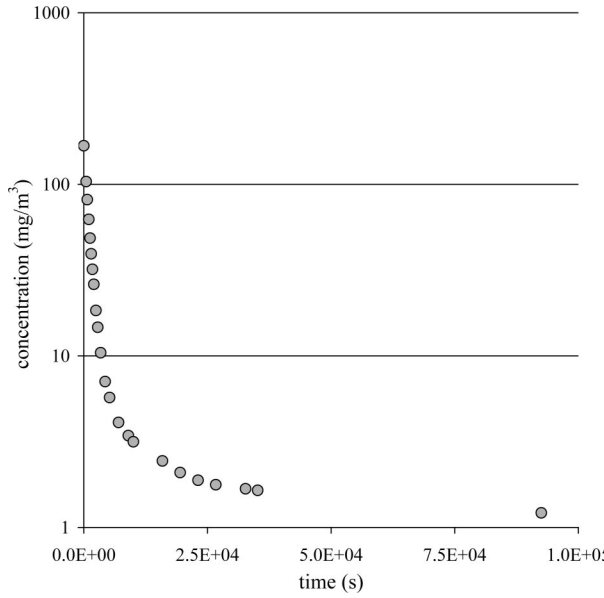

Figure 3. Adsorption kinetics of THT onto ACFC; $T = 25 \pm 0.2$ °C; $C_0 = 168$ (mg m^{-3}); $m = 250$ mg.

From the standpoint of batch adsorption capacities, the ACFC FM30K shows more interesting opportunities for THT removal in natural gas than GAC. These first promising batch results for the ACFC have to be validated by the kinetic investigation.

Adsorption Kinetics. The initial adsorption coefficient γ, the external film mass-transfer coefficient k_sA, and the internal diffusion coefficient of Weber K_W were assessed from the adsorption kinetic curves and are presented in Table 2. The adsorption kinetic curve of THT onto ACFC is shown in Figure 3.

The ACFC shows an initial adsorption coefficient γ, which is double that of the GAC, and also has the highest external film mass transfer. The ACFC is composed of fibers of small diameter close to 10 μm (Figure 1), which induces a higher external surface area compared to GAC and thus a faster film diffusion. This higher external area of the ACFC greatly influences the initial adsorption kinetics as well; thus, the ACFC obtains the highest value for the parameter γ. The grain diameter influences the initial adsorption kinetic. The smaller the grain, the higher the initial adsorption kinetic observed for these materials. However, the grain diameter used in this study has a typical range size (0.8−1.4 mm) for the filtering bed in the industrial process gas treatment. A smaller grain size would imply a significant increase of the pressure drop for the filtering bed.

The internal diffusion coefficient K_W is of the same order of magnitude for the adsorbents. This observation is due to the fact that adsorbents present high microporosity. Adsorbates reach adsorption sites through micropores without additional diffusion resistance of mesopores, which is usually the rate-controlling step in the case of adsorbents.[30] The slightly higher value in the case of the NC60 may be explained by the influence of the favorable chemical structure of the adsorbent already mentioned in the equilibrium adsorption isotherm investigation.

To summarize our adsorption investigations, the ACFC exhibits kinetic advantages and better adsorption properties than the GAC for the adsorption of THT in a natural gas matrix. Thus, the regeneration and adsorption−desorption studies were conducted specifically on the ACFC.

Adsorption−Desorption Cycles. The thermogravimetric desorption curves of a blank and a saturated ACFC sample by natural gas are shown in Figure 4. The blank sample was

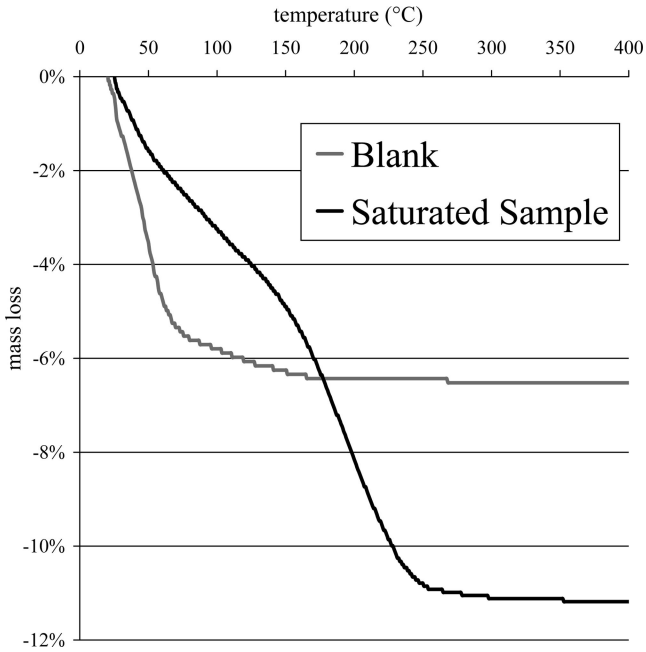

Figure 4. Thermogravimetric desorption of ACFC; $m = 20$ mg; $dT/dt = 5$ °C min^{-1}.

repeated twice. The observed mass losses were 6.4 and 6.6%. Figure 4 shows the 6.4% mass loss. Two samples, saturated the same way, reported the mass losses of 11.2 and 12.1%. For reasons of visiblity, only the 11.2% mass loss is shown. In both saturated sample cases, samples were regenerated at 99% of their virgin dry mass.

The blank ACFC desorption curve could be divided into two different parts. The first one, from ambient temperature to 130 °C, corresponds to water desorption. For the saturated sample, this first part does not correspond to water desorption, because only traces of water remain in natural gas; it represents the low-energy-bonded compound desorption, which may include adsorbed THT. Then, from 160 °C, the saturated sample desorbs more strongly bonded adsorbates until 240 °C. This may be explained by the release of compounds located in the pores of smaller diameter in the ACFC. Thus, the thermogravimetric experiments confirm the possibility of desorbing THT from the ACFC.

The desorption temperature is assessed in the range of 160−240 °C. The maximal desorption temperature is evaluated at 240 °C to ensure fast regeneration of the ACFC compared to a regeneration at 160 °C. These first observations on the desorption behavior of THT from the FM30K were now tested in cycles of adsorption−desorption. The adsorption−desorption capacity during cycles versus the desorption temperature is shown in Figure 5.

First of all, the cycle experiment confirms the potential of the AFCF to carry out multiple cycles of adsorption−desorption of THT from the natural gas matrix without a significant decrease in its adsorption capacity. The first cycle adsorption capacity of the ACFC in the continuous process is of the same order of magnitude (about 10% higher) as the predicted adsorption capacity from the batch results for the same THT gas-phase concentration. Hence, batch investigations reliably gave the magnitude of the THT adsorption capacity for the continuous process certainly because the natural gas matrix was respected.

Table 3 shows the adsorption results reported in the literature and those obtained in this study. Except for the adsorbents studied by Roh,[14] which exhibit a very high adsorption capacity,

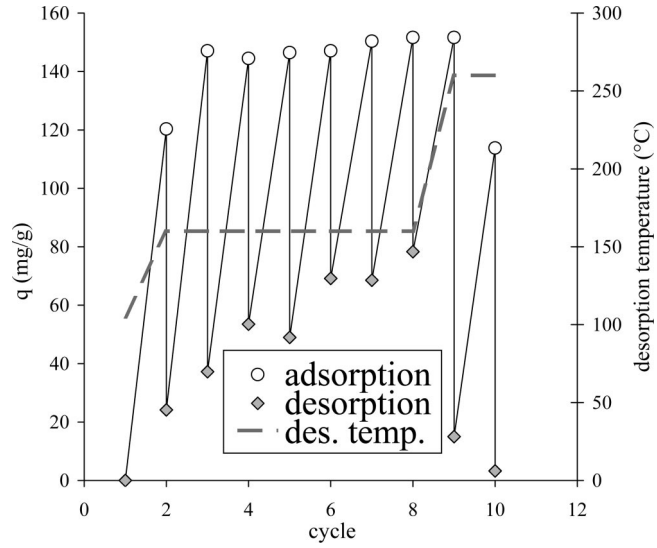

Figure 5. Adsorption−desorption cycles onto ACFC of THT in natural gas; desorption time: overnight for about 13 h.

the FM30K results are of the same order of magnitude as the most efficient zeolites.

Although the ACFC showed attractive results in the continuous removal of THT from the natural gas, the adsorption capacity was not constant during the adsorption−desorption cyclical process. Until the eighth cycle, desorption was fixed at 160 °C; thus, regeneration was incomplete. This is shown by the increasing amount of sulfur compound adsorbed onto the ACFC after desorption, represented by gray diamonds in Figure 5. After the second cycle, the final adsorption capacity, represented by white circles, reached a stable value. Both phenomena lead to a decrease in the ACFC adsorption capacity, explained by the incomplete regeneration of the material. Therefore, cycles at 260 °C desorption temperature were carried out, resulting in an adsorbed amount after desorption close to zero. Thus, hypotheses drawn from the thermogravimetric measurements on the desorption temperature were confirmed. The material is of definite interest in a global desulfurization process. However, it should be noted that the high-temperature regeneration decreases the final adsorption capacity. The material can resist higher temperatures than the one investigated; thus, this observation may be due to chemical modification of the material or byproduct formation at the surface of the ACFC, which may perturb the adsorption sites or pore access for the THT. Therefore, experiments of desorption at specific temperatures where the gas phase is monitored by GC/MS were set up to investigate the byproduct formation phenomenon. In addition, the chemical modification of the material surface was investigated using scanning electron microscopy coupled with X-ray diffraction.

Byproduct Formation during Desorption. The ACFC sample saturated with natural gas (containing THT) was desorbed at 60, 100, 140, 180, and 210 °C. Because of the assumptions from the thermogravimetric measurements shown in Figure 4, from 100 to 140 °C, the desorption of the low-energy-bonded compounds is investigated, whereat at 180 and 210 °C, the stronger bonded compounds are expected. Aliquots of the gas phase were withdrawn and automatically injected into the GC/MS apparatus to monitor their composition. The presence of thiophene is indicated at desorption temperatures higher than 100 °C. The chromatogram and the mass spectra of the desorption at 100 °C are reported in Figures 6 and 7.

The chromatogram in Figure 6 contains two separate peaks. The extracted mass chromatogram at m/z 84 shows a significant

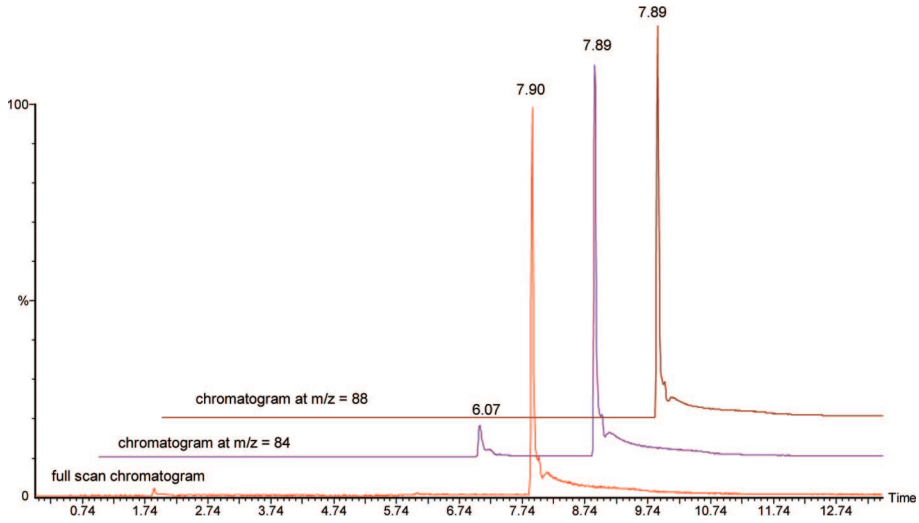

Figure 6. Chromatogram of the gas phase during desorption at 100 °C of ACFC.

Table 3. Uptake Capacity of Different Adsorbent Materials

adsorbent	condition	adsorbate	concentration (ppm)	adsorbent capacity (mmol g^{-1})	references
zeolite after regeneration	dynamic	TBM + DMS	3	0.7	Satakowa[13]
zeolite	static	TBM	275	3.3	Satakowa[13]
ZnO	dynamic	H_2S	8	0.07	Novochinski[15]
AC	dynamic	THT + TBM	3	25.8	Roh[14]
zeolite	dynamic	THT + TBM	3	117	Roh[14]
zeolite	dynamic	THT + TBM	80	1.28	Ko[9]
ACFC	static	THT	56	2.3	present study
ACFC	dynamic	THT	14	1.1	present study

peak with a retention time at 6.07 min, which, according to the database, is an excellent match to the compound thiophene. The second peak matches THT. Its retention time is 7.89 min, with significant response for the extracted mass chromatogram at *m*/*z* 88. All spectra from 100 °C exhibit the occurrence of thiophene in the gas phase, although the natural gas is thiophene-free (tested by the GC/MS apparatus). Hence, it can be assumed that this reaction occurs at a temperature close to 100 °C because only traces of thiophene are measured at this temperature. The validation of thiophene formation from THT was performed on an ACFC sample saturated with pure commercial THT and desorbed at 180 °C.

The dehydrogenation of THT reported by Desikan and Amberg[23] involves the formation of thiophene, butene, butane, and hydrogen sulfide among the byproduct. Authors who have investigated hydrogen sulfide adsorption onto ACFC[31,32] pointed out the oxidation reaction between hydrogen sulfide and oxygen-containing sites at the activated carbon surface to obtain finally elemental sulfur onto the ACFC. Hence, according to the literature, elemental sulfur should be present on the ACFC. SEM with X-ray spectrometer experiments was performed to confirm the undoubted presence of elemental sulfur on the surface of the sample exposed to the 10-cycle adsorption−desorption procedure after its last desorption at 300 °C. The average elemental sulfur concentration in the ACFC sample was measured at 1.24% by weight with a 0.09 standard deviation after the 10-cycle adsorption−desorption experiment, whereas for a blank sample of ACFC, the elemental sulfur concentration was insignificant (less than 0.1%). The occurrence of elemental sulfur on ACFC is explained by the oxidation of hydrogen sulfide formed by the dehydrogenation of THT. The reaction path of the dehydrogenation of THT advanced by Desikan and Amberg[23] is rather complex and partially unknown, but our experimentally determined byproduct is mentioned. Thus, a summarized degradation pathway in our case coupling the results of Desikan and Amberg[23] and Le Leuch et al.[31] is presented in Figure 8.

In Figure 8, the compounds in square brackets are reported in the literature, although they have not been monitored in this study. Even though the butane and butadiene have not been experimentally measured, they may explain the first part of the thermogravimetric curve of the saturated sample in Figure 4 because they should desorb before THT or thiophene as a result of their difference of vapor pressures. Thus, the observations of the main byproduct are confirmed by the literature and highlight the reaction between THT and activated carbon to form thiophene, triggering the presence of elemental sulfur on the ACFC. This presence may explain the small loss of adsorption capacity observed after the 10th cycle of adsorption−desorption of THT onto the ACFC. Indeed, because elemental sulfur has a crystalline structure (S_8^0), its desorption from activated carbon is rather complicated to achieve.

Such results highlight the necessity for prior investigations before regeneration by heating. The formation of thiophene does not represent a barrier to the regeneration process contrary to the elemental sulfur deposit on the ACFC, which may significantly decrease its adsorption capacity. However, the elemental sulfur formation is dependent upon the regeneration temperature because it is a catalytic reaction. Hence, ACFC regeneration at temperatures close to 160 °C results in a very low reaction yield of elemental sulfur. A compromise between incomplete regen-

(31) Le Leuch, L.; Subrenat, A.; Le Cloirec, P. *Langmuir* **2003**, *19*, 10869–10877.

(32) Le Leuch, L.; Subrenat, A.; Le Cloirec, P. *Environ. Technol.* **2005**, *26*, 1243–1254.

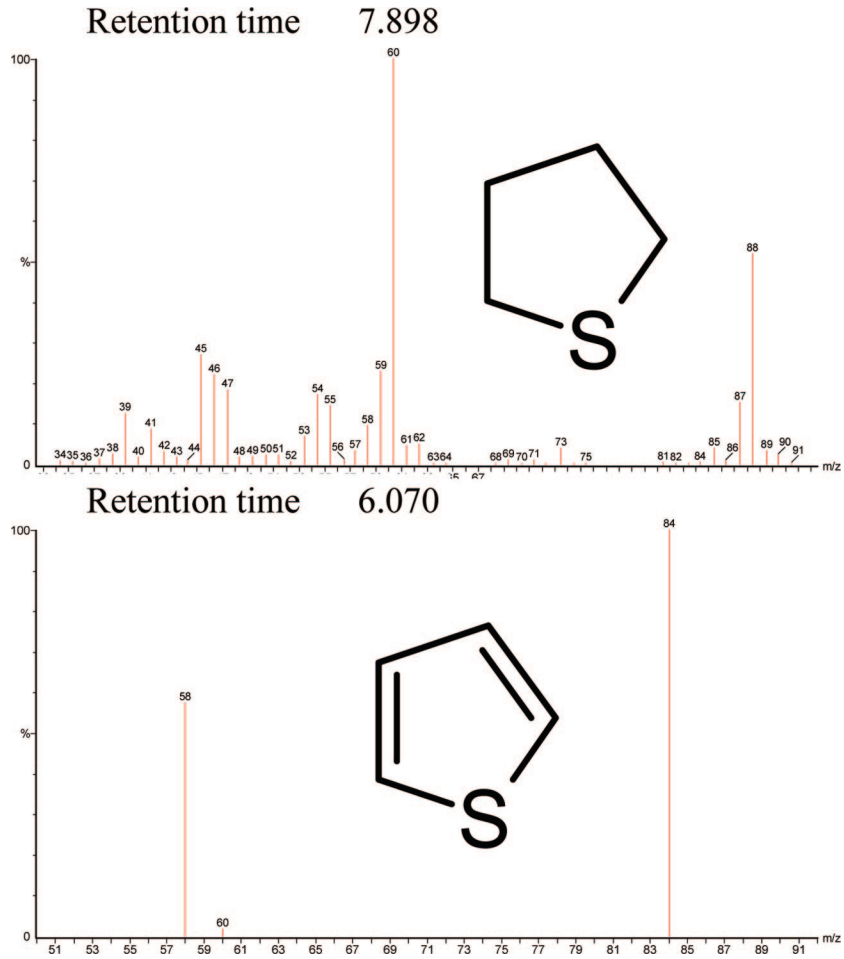

Figure 7. Mass spectra of THT (above) and thiophene (below) desorbed from ACFC at 100 °C.

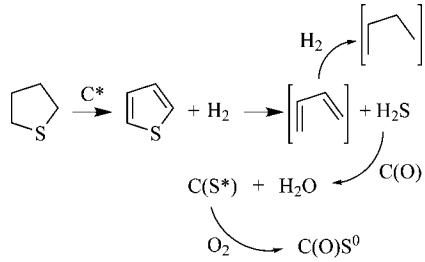

Figure 8. Potential pathway and byproduct formation during THT desorption from ACFC.

eration and elemental sulfur production may be determined to optimize the process.

Conclusion

The purpose of this work was to investigate the ACFC adsorption/regeneration capacity of THT from natural gas. This contributes to the use of such material for desulphurization prior to fuel cell application based on natural gas as the primary fuel. The commercial ACFC was compared to two regular GAC for THT adsorption capacity and kinetic uptake in batch reactors. Results showed that the ACFC provided a higher adsorption velocity than the GAC. The initial adsorption coefficient of ACFC was found to be double those obtained with GAC. The external surface area developed by the ACFC explains such behavior.

Langmuir's equation was applied, and model parameters were computed. The ACFC presented the highest adsorption capacity for the magnitude of THT concentration in natural gas. Adsorption behavior of materials was explained by their physical properties. From the standpoint of batch experiments, the ACFC surpasses the GAC for desulfurization of natural gas and thus justifies the interest of ACFC for a complete process.

Because ACFC presents a valuable regeneration process by the Joule effect, the thermal regeneration of a saturated ACFC sample by THT from natural gas was studied. Thermogravimetric measurements placed the regeneration temperature between 160 and 250 °C, with a complete regeneration in the range from 230 to 250 °C to desorb strongly bonded compounds. The GC/MS part highlighted the reactivity of THT during the thermal regeneration to form thiophene at temperatures higher than 100 °C, triggering hydrogen sulfide formation. Hydrogen sulfide reacted with oxygen-containing sites of the ACFC, leading to elemental sulfur formation at the ACFC adsorption site, which decreased the adsorption capacity of the ACFC. This last point requires particular attention in further studies to assess the optimal regeneration temperature by the Joule effect.

These results confirm the interest of considering ACFC for desulfurization of natural gas, even though the literature mostly reports the alternative option, using zeolite to realize this adsorption treatment.

Acknowledgment. The authors thank Pica (Saint-Maurice, France) and Charcoal Cloth International (U.K.) for supplying activated carbon material.

Nomenclature

AC = activated carbon
ACFC = activated carbon fiber cloth
ARE = average relative error = $(1/n)\sum_{i=1}^{n}[(q_e - \hat{q}_e)/q_e]_i$

b = Langmuir constant (m^3 mg^{-1})
C_e = equilibrium gas-phase concentration (mg m^{-3})
C_0 = initial gas-phase concentration (mg m^{-3})
GAC = granular activated carbon
γ = initial adsorption kinetic coefficient (m^3 g^{-1} s^{-1})
HDS = catalytic hydrodesulfurization process
HYBRID = $[1/(n - p)]\sum_{i=1}^{n}[(q_e - \hat{q}_e)/q_e]_i$
K_{ABT} = Adam, Bohart, and Thomas' adsorption kinetic constant (m^3 mg^{-1} s^{-1})
K'_{ABT} = Adam, Bohart, and Thomas' desorption kinetic constant (s^{-1})
k_sA = external film mass-transfer coefficient (m^3 s^{-1})
K_W = Weber's internal diffusion coefficient (mmol m^{-3} $s^{-0.5}$)
m = adsorbent mass (g)
ppm = part per million
q_e = equilibrium solid-phase concentration (mg g^{-1})
q_m = maximum adsorption capacity (mg g^{-1})
$r^2 = \sum_{i=1}^{n}(\hat{q}_e - \bar{q}_e)_i^2/[\sum_{i=1}^{n}(\hat{q}_e - \bar{q}_e)_i^2 + \sum_{i=1}^{n}(q_e - \bar{q}_e)_i^2]$
S_{BET} = surface area according to the BET theory (m^2 g^{-1})
SEM = scanning electron microscopy
s_{RE} = standard deviation of the relative error = $(\sum_{i=1}^{n}\{[(q_e - \hat{q}_e)/q_e]_i - ARE\}_i^2/(n - 1))$
THT = tetrahydrothiophene
V = batch reactor volume (m^3)

EF800757U